Control of 2dof Planar Parallel Manipulator Using Backstepping Approach

Mustapha. Litim * **Abdelhafid. Omari** **
Mohamed El Amine. Larbi ***

* *University of Sciences and Technology MB, Faculty of Electrical Engineering, Automatic Control Department, BP 1505 Oran El MNaouer, Algeria, (e-mail: lit_ldee@yahoo.fr).*
** *University of Sciences and Technology MB, Faculty of Electrical Engineering, Automatic Control Department, BP 1505 Oran El MNaouer, Algeria, (e-mail: o_albdelhafid@hotmail.com)*
*** *University of Sciences and Technology MB, Faculty of Electrical Engineering, Automatic Control Department, BP 1505 Oran El MNaouer, Algeria, (atar2506@yahoo.fr)*

Abstract: In this paper, dynamic equations of motion for a 2DoF parallel robot manipulator including structured and unstructured uncertainties are considered. The application of Backstepping technique for trajectory tracking in presence of parameter uncertainties in mass variation is studied. The advantage of this control technique is that it imposes the desired properties of stability by fixing initially the candidate Lyapunov functions, then by calculating the other functions in a recursive way. Simulation results are presented in order to evaluate the tracking performance and the global stability of the closed loop system. Obtained results show the effectiveness of the proposed controller for 2DoF parallel robot.

Keywords: Nonlinear control, Parallel manipulators, Lyapunov stability, backstepping control.

1. INTRODUCTION

Parallel robots are closed-loop mechanisms where all of the links are connected to the ground and the moving platform at the same time. They have high rigidity, load capacity, precision and especially structural stiffness, since the end effectors is linked to the movable platform at several points Kang et al. (2001), Kang and Mills (2001), Merlet (2001), Tsai (1999), and Uchiyama (1993). Despite of their advantages, parallel manipulators have also some drawbacks, such as limited workspace and complex kinematic issues caused by the presence of multiple closed loop chains and singularities. Two categories of parallel manipulators exist, spatial and planar robot. The first category composes of the spatial parallel robots that can translate and rotate in the three dimensional space. Gough-Stewart platform Gough (1956), Stewart (1965), one of the most popular spatial manipulator, is extensively preferred in flight simulators. The planar parallel robot which comprises of second category, translates along the x and y axes, and rotates around the z axis, only. Although planar parallel manipulators are increasingly being used in industry for micro or nano positioning applications Hubbard et al. (2001), and in industrial high speed applications Weck and Staimer (2002). In this paper, we will discuss the motion control of a planar parallel robot known as Biglid with two degrees of freedom (DoF) Vermeiren et al. (2012), Cheung and Hung (2005), Pierrot et al. (2011). This type of parallel robot is used in the manufacturing industry of electronic products, as pick and place applications Vermeiren et al. (2012). The dynamics modelling of parallel manipulators are more difficult because of the presence of kinematic close loop than their serial counterparts. Therefore selection of an efficient kinematic modelling convention is very important for simplifying the complexity of the dynamics problem in planar parallel manipulators. Many researchers worked on the dynamic modelling of parallel robots Khalil and Ibrahim (2007), Staicu et al. (2007) and Staicu (2009). Regarding the parallel robots control, many methods are studied in the literature. They can be classified into classical control methods, modern and intelligent control methods. The classical methods, such as simple PD and PID linear control, are easily implemented but not suited for nonlinear system. Modern control methods like motion control are simple in the structure and have better performance in control. The intelligent control methods can prove the best control performance but it needs a lot of experience and is always hard to design. In recent years many researchers are worked on the intelligent control method for nonlinear mechanical systems Martynyuk (2000), Yang et al. (2008), such as adaptive control Zhu et al. (2009), fuzzy control Guo and Woo (2003), Yang et al. (2008), TS disruptor Vermeiren et al. (2012), Sliding mode control Mustapha et al. (2014) and computed torque Yang et al. (2007). These types of controller work very well when all dynamic and physical parameters are known, but when the manipulator has variation in dynamic parameters, the controller has no acceptable performance Vermeiren et al. (2012). Sliding mode control, which is a new method, can be a solution, but some bounds on system uncertainties must be pre estimated Le et al. (2013). In this paper, a new contribution based on backstepping approach is proposed to control parallel robot in the Cartesian space. This approach is based on the direct dynamic model in Cartesian space. Backstepping method could be utilized for nonlinear position control in robotic systems. It guarantees asymptotic stability in tracking of desired position and speed trajectories, while preserving useful system nonlinearities. Backstepping control has been used for several applications such as Full Control of a Quadrotors Bouabdallah and Siegwart (2007) Backstepping-based control of rigid robots including actuators has been studied in Su and Stepanenko (1997) and Control of a brush DC motor in Dawson et al. (1994). The remainder of this paper is organized as follow. In Section2, the dynamic model of 2-DoF parallel manipulator is formulated in the Cartesian space. In Section3, Backstepping controller is developed and applied to the direct dynamic model of robot in Cartesian space. Section4 presents simulation results of the proposed controller. Finally, some conclusions are presented in the closing section.

2. DYNAMICS MODELING OF BIGLIDE PARALLEL ROBOT

2.1 Kinematic and geometric analysis

For the geometric and kinematics modeling of a Biglide parallel manipulator, the following conventions are used according to Vermeiren et al. (2012). The manipulator provides 2DOF of translation on the XY plane, the positioning of end effector is represented by operational variables (x, y) driven by two prismatic active joints (q_1, q_2) in the same X axis.
The operational vector is then written as follow:

$$P = [x \ y]^T \tag{1}$$

The generalized joint variable vector is:

$$q = [q_1 \ q_2]^T \tag{2}$$

The mechanism has two constant length struts with moveable foot points Figure 1. Both struts have the same lengtha. The relationship between both coordinate vectors is written with kinematic loop-closure constraints Figure 1:

$$\Phi(P,q) = 0, \Phi(P,q) = \begin{pmatrix} (x-q_1)^2 + y^2 - a^2 \\ (q_2 - x)^2 + y^2 - a^2 \end{pmatrix} \tag{3}$$

The Inverse geometric model (IGM) formula is given by:

$$q = g\,(P) \tag{4}$$

with

$$g(P) \equiv \begin{pmatrix} x - C(y) \\ x + C(y) \end{pmatrix}, C\,(y) \equiv \sqrt{a^2 - y^2} \tag{5}$$

The direct geometric model (DGM) can be derived from (4):

$$P = g^{-1}\,(q) \tag{6}$$

with

$$g^{-1}(q) = \begin{pmatrix} \dfrac{q_1 + q_2}{2} \\ \sqrt{a^2 - \dfrac{(q_1+q_2)^2}{4}} \end{pmatrix} \tag{7}$$

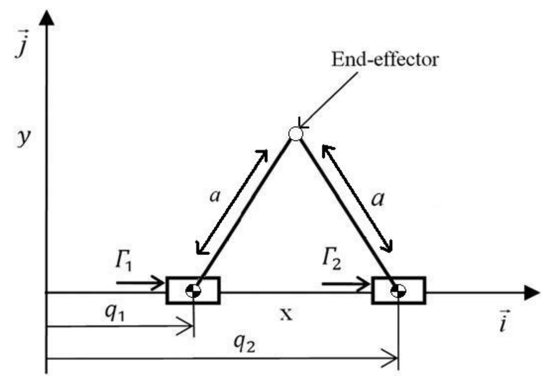

Fig. 1. kinematic schemes of Biglide robot.

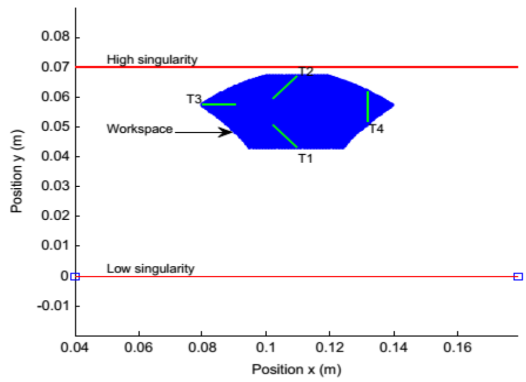

Fig. 2. Workspace and trajectories: $(T1)$ Low trajectory, $(T2)$ High trajectory, $(T3)$ Left trajectory, and $(T4)$ Right trajectory.

The relation between the joint space and the operational space is conveniently described by two Jacobian matrices $J_p(P,q)$ and $J_q(P,q)$ is given as:

$$J_p(P,q)\dot{P} = J_q(P,q)\dot{q} \tag{8}$$

The parallel singularities occur when the Jacobian matrix J_p is rank deficient. The Biglide has two parallel singularities: Vermeiren et al. (2012)
• High singularity: $q_1 = q_2 = x$, the struts are superposed and $y = 0.07$, Figure 2.
• Low singularity: $y = 0$, the struts are aligned, Figure 2
The kinematic relationship between end-effector velocities and joint velocities is computed by differentiating (3) with respect to time:

$$J_p(P,q)\dot{P} = J_q(P,q)\dot{q} with J_p(P,q) = \begin{bmatrix} x - q_1 & y \\ x - q_2 & y \end{bmatrix}$$

$$J_p(P,q) = \begin{bmatrix} x - q_1 & 0 \\ 0 & x - q_2 \end{bmatrix} \tag{9}$$

2.2 Dynamic Model

The dynamics equations of the Biglide in operational space are given as follows:

$$\Gamma = M(P)\ddot{P} + N(P,\dot{P}) \tag{10}$$

with

$P = [x, y]^T$, $M(P)$ is the inertial matrix given as follow:

$$M(P) = \begin{pmatrix} m_1 + \frac{1}{2}(m - \lambda_1 + \lambda_2) \ f_1(P) \\ m_2 + \frac{1}{2}(m - \lambda_2 + \lambda_1) \ f_2(P) \end{pmatrix} \tag{11}$$

with

$$\lambda_{1,2} = ms_{1,2}/a$$

$$\begin{cases} f_1(P) = [(2m_1 - 3\lambda_1 - \lambda_2)y^2 + mC(y)^2 + J_1 \\ J_2]/(2C(y) \times y) \\ f_2(P) = -[(2m_2 - 3\lambda_2 - \lambda_1)y^2 + mC(y)^2 + J_1 \\ +J_2]/(2C(y) \times y) \end{cases}$$

$$N(P, \dot{P}) = N(y, \dot{y}) + p(y)$$

$N(y, \dot{y})$ is a coriolis / centripetal matrix can be written as:

$$R(y, \dot{y}) = \begin{bmatrix} r_{11} \ r_{12} \\ r_{21} \ r_{22} \end{bmatrix} \tag{12}$$

$$\begin{cases} r_{11} = r_{12} = 0 \\ r_{12} = -[(2m_1 - 3\lambda_1 - \lambda_2)y^2 + (2m_1 - 3\lambda_1 - \lambda_2) \\ C(y)^2 + J_1 + J_2]\dot{y}/(2C(y))^3 \\ r_{22} = [(2m_2 - 3\lambda_2 - \lambda_1)y^2 + (2m_2 - 3\lambda_2 - \lambda_1) \\ C(y)^2 + J_1 + J_2]\dot{y}/(2C(y))^3 \end{cases}$$

$p(y)$ is a vector containing gravity torques can be written as:

$$p(y) = \begin{pmatrix} (gC(y)(m + \lambda_1 + \lambda_2))/2y \\ (-gC(y)(m + \lambda_1 + \lambda_2))/2y \end{pmatrix} \tag{13}$$

3. CONTROLLER DESIGN

Backstepping is a recursive procedure that guarantees asymptotic stability by interlacing the choice of a Lyapunov function with the design of feedback control. Backstepping method could be utilized for nonlinear position control in robotic systems. It guarantees asymptotic stability in tracking of desired position and speed trajectories, while preserving useful system nonlinearities. In this section the control low based on Backstepping approach is applied on the direct dynamic model in operational space of 2DoF planar parallel manipulator Biglid type. The results obtained by Backstepping controller were compared to results of PID and computed torque control (CTC) presented by Vermeiren et al. (2012).

3.1 PID controller

The control law based on PID controller in the joint space is given by the following expression:

$$\Gamma = G(s)\varepsilon_q \tag{14}$$

Where Eq.(3) of invers geometric model is used to compute the desired joint positions.

$$q^d = g\left(P^d\right) \tag{15}$$

with $\varepsilon_q = q^d - q$ and the PID controller $G(s) = g_p + g_d s + g_i/s$ Gain g_p, g_d, g_i are $(n_{dof} \times n_{dof})$ positive definite diagonal matrices.

For PID control in the operational space, the control law is obtained by transforming the operational space error signal into the joint space as follows:

$$\Gamma = J^T G(s)\varepsilon_p \tag{16}$$

with $J = J_p^{-1} J_q$ and the PID controller $G(s) = g_p + g_d s + g_i/s$.

The error vector is given by

$$\varepsilon_P = P^d - P \tag{17}$$

3.2 CTC controller

Computed torque controller (CTC) is nonlinear controller which it widely used in control of parallel robots. The central idea of Computed torque controller (CTC) is feedback linearization so, originally this algorithm is called feedback linearization controller. This controller works very well when all dynamic and physical parameters are known but when the robot manipulator has variation in dynamic parameters, in this situation the controller has no acceptable performance.

Using the differential flatness property of the model (10) a control law that linearizes and decouples the equations (n_{dof}decoupled linear systems) can be derived. Therefore, the robot is resumed in to a double integrator equation in the operational space:

$\lambda(t) = \ddot{P}$ Joint forces Γ obtained from inverse dynamic model (10) depend on the new control input $\lambda(t)$ and the operational position $P(t)$

They are computed as follows:

$$\Gamma = \hat{M}(P)\lambda + \hat{N}(P, \dot{P}) \tag{18}$$

Typical choices for λ are linear controllers such as PID with acceleration feedforward:

$$\lambda = \ddot{P}^d + G(s)\varepsilon_p \tag{19}$$

3.3 Backstepping controller

From equation (10), the direct dynamic model in operational space of Biglid robot is presented as follow:

$$\ddot{P} = M(P)^{-1}[\Gamma - N(P, \dot{P})] \tag{20}$$

with

$P = [x, y]^T$ is x and y vector positions of the end-effector.

$\Gamma = [\Gamma_1 \Gamma_2]^T$ is a vector of input control signal.

In order to apply Backstepping method, define $x_1 = P, x_2 = \dot{P}$ using (20), we obtain:

$$\dot{x}_2 = \ddot{P} = M^{-1}(P)[\Gamma - N(P, \dot{P})] \tag{21}$$

For the first step we consider the tracking error as follow:

$$e_1 = x_{1d} - x_1 \tag{22}$$

Its time derivative is then:

$$\dot{e}_1 = \dot{x}_{1d} - \dot{x}_1 \tag{23}$$

Then we use the Lyapunov theorem by considering the Lyapunov function e_1 positive definite and its time derivative negative semi-definite:

$$V_1 = \frac{1}{2} e_1^T e_1 \tag{24}$$

Its time derivative is

$$\dot{V}_1 = e_1^T \dot{e}_1 = e_1^T(\dot{x}_{1d} - \dot{x}_1) = e_1^T(\dot{x}_{1d} - x_2) \quad (25)$$

The stabilization of e_1 is obtained by introducing a virtual control input x_2:

$$x_2 = \dot{x}_{1d} + k_1 e_1, (k_1 > 0) \quad (26)$$

with $k_1 \in R^{2\times 2}$ is a positive definite matrix. The equation (25) is then:

$$\dot{V}_1 = -e_1^T k_1 e_1 \quad (27)$$

Let us proceed to a variable change by making:

$$e_2 = x_{2d} - x_2 = k_1 e_1 + \underbrace{\dot{x}_{1d} - x_2}_{\dot{e}_1} \quad (28)$$

hence $\dot{e}_1 = e_2 - k_1 e_1$

For the second step we consider the augmented Lyapunov function:

$$V_2 = \frac{1}{2}\sum_{i=1}^{2} e_i^T e_i \quad (29)$$

Its time derivative is then:

$$\dot{V}_2 = e_1(e_2 - k_1 e_1) + e_2(k_1\dot{e}_1 + \ddot{x}_{1d} - \dot{x}_2) \quad (30)$$

$$\dot{V}_2 = -k_1 e_1^2 + e_2(e_1 + k_1\dot{e}_1 + \ddot{x}_{1d} - \dot{x}_2) \quad (31)$$

For the system to be stable it is necessary that $\dot{V}_2 < 0$. From Equation (31) we have

$$(e_1 + k_1\dot{e}_1 + \ddot{x}_{1d} - \dot{x}_2) = -k_2 e_2 \quad (32)$$

where $k_2 > 0$

$$\dot{x}_2 = e_1 + k_1\dot{e}_1 + \ddot{x}_{1d} + k_2 e_2 \quad (33)$$

$$M^{-1}(x_1)[\Gamma - N(x_1, x_2)x_2] = e_1 + k_1\dot{e}_1 + \ddot{x}_{1d} + k_2 e_2 \quad (34)$$

The control input Γ is then extracted as:

$$\Gamma = N(x_1, x_2)x_2 + M(x_1)\left[e_1 + k_1\dot{e}_1 + \ddot{x}_{1d} + k_2 e_2\right] \quad (35)$$

Taking equation (28) for e_2 and substituting in (35), we have:

$$\Gamma = N(x_1, x_2)x_2 + M(x_1)\left[\dot{e}_1(k_1 + k_2) + \ddot{x}_{1d} + e_1(1 + k_1 k_2)\right] \quad (36)$$

$\Gamma = [\Gamma_1, \Gamma_2]$ is the vector of control signal input.

$x_1 = P = [x, y]$ is the position vector.

$k_1 = \begin{pmatrix} k_{1x} & 0 \\ 0 & k_{1y} \end{pmatrix}$ is a diagonal positive matrix gain of controller.

$k_2 = \begin{pmatrix} k_{2x} & 0 \\ 0 & k_{2y} \end{pmatrix}$ is a diagonal positive matrix gain of controller.

4. SIMULATION RESULT

This section presents the performance evaluation of the proposed Backstepping controller. The reference trajectory tracking is a 5^{th}order polynomial interpolation. The

Table 1. Parameters model of Biglide parallel robot

Parameters	Values
Strut length (m) a	0.07
Mass (kg)	
m	0.034
$m1$	0.8040
$m2$	0.7940
First moment of links (kgm)	
ms_1	0.0045
ms_2	0.0043
Second moment of links (kgm^2)	
J_1	222.643×10^{-4}
J_2	2.539×10^{-4}
Gravity acceleration (ms^2)	
g	9.81
Additional parameter for the simulation model Mass (kg)	
λm	0.816

2DoF Biglid parallel robot parameters used in simulation are listed in Tab. 1.

Two cases are considered in the simulation test. In the first case, trajectory tracking with no parameter uncertainties is considered. When for the second case, the system is simulated with parameter uncertainties. The structured uncertainties are considered for a mass variation of the end-effector corresponding to $\Delta m = 0.816kg$; of course no uncertainty corresponds to $\Delta m = 0$. Simulation results of PID, CTC and Backstepping controllers are presented in Figure 3 and Figure 4, Figure 7 and Figure 8 for the trajectories T1 (near work space low boundary) and Figure 5 and Figure 6, Figure 9 and Figure 10 for T2 (near work space high boundary), for each figure trajectories, parts (a) and (b) present the set Point and the response along x and y axes and parts (c) and (d) present the control input of both actuators. Note also that Figure 3 and Figure 4 , Figure 5 and Figure 6 are without mass variation $\Delta m = 0$ where as Figure 7 and Figure 8, Figure 9 and Figure 10 uses a mass variation $\Delta m = 0.816kg$; . The mass variation is used to test the robustness and effectiveness of proposed Backstepping controller, and compared to results of PID and CTC controllers Vermeiren et al. (2012).

4.1 Discussion of simulation results

Un-modelled dynamics such as elastic joints and Stribeck friction appear in the simulation model to provide a more realistic behaviour is presented in appendix. Notice that two resonant modes are added in the simulation model simulating the elastic joint such as the lower value of the resonant frequency is $\omega_r = 29rad/s$

BS: Backstepping Control (36);
CTC: Computed Torque Control, Vermeiren et al. (2012);
PID: proportional integral derived, Vermeiren et al. (2012);

In the former case, $\Delta m = 0$ going from the best to the worst; The Backstepping and CTC Controller show a good capability of response. Whereas PID shows important overshoot. Based on Figure 7 and Figure 8, Figure 9 and Figure 10 by comparing response trajectory with mass variation of platform $\Delta m = 0.816kg$ Backstepping

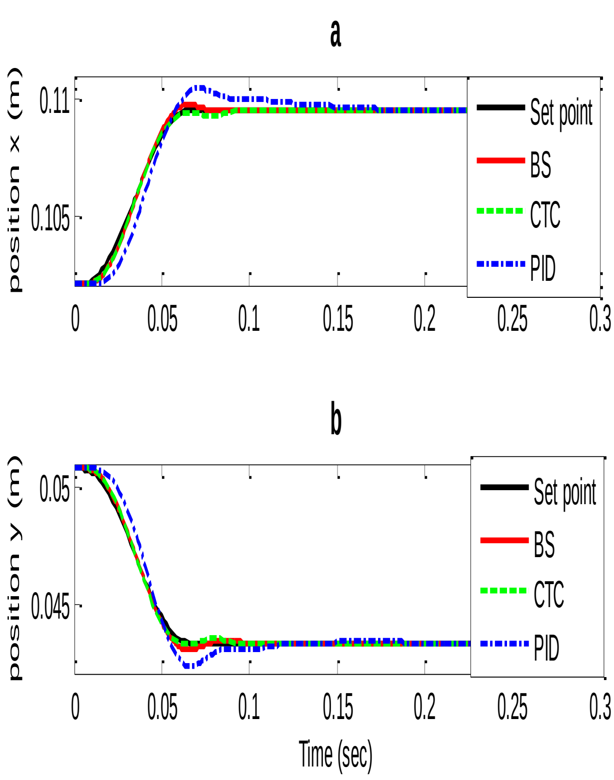

Fig. 3. Control schemes for low trajectory (T1) and $\Delta m = 0$

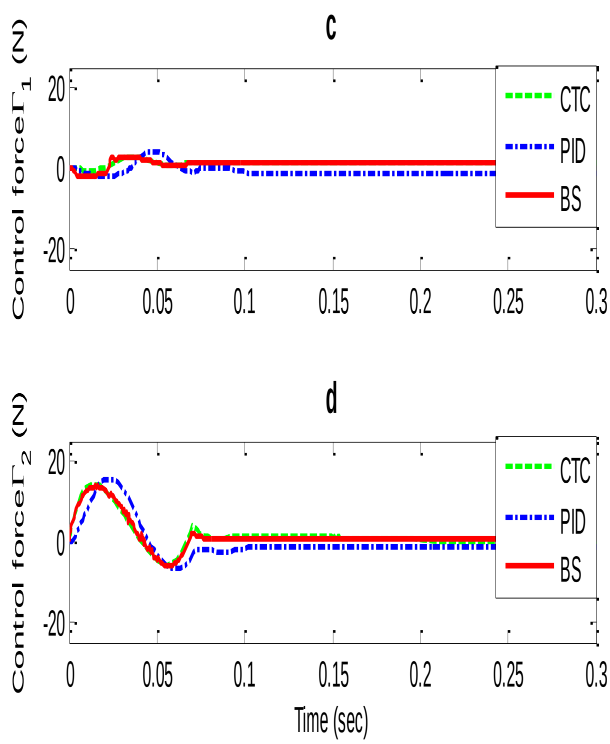

Fig. 4. Control schemes for low trajectory (T1) and $\Delta m = 0$

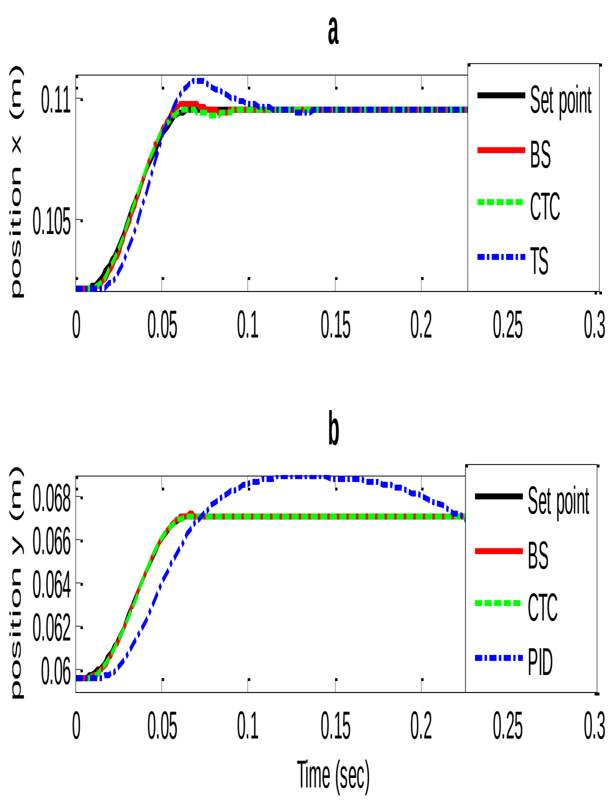

Fig. 5. Control schemes for high trajectory (T2) and $\Delta m = 0$

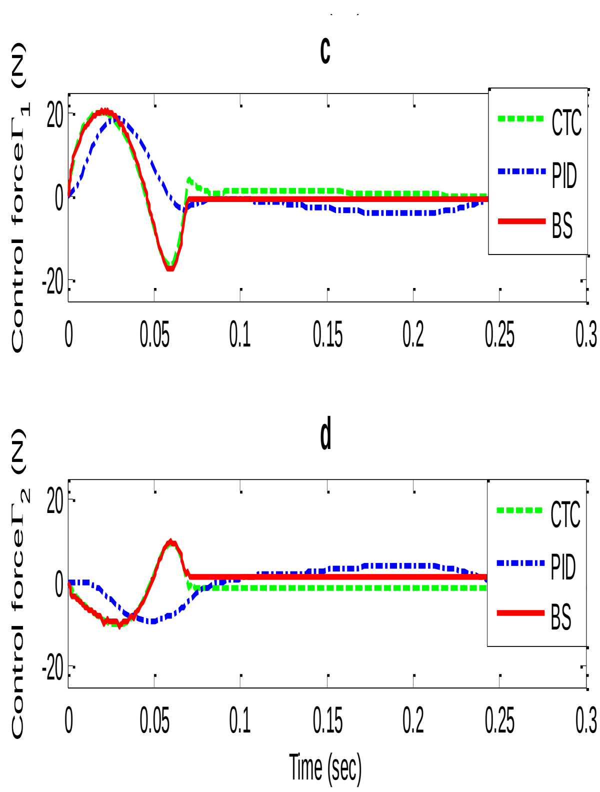

Fig. 6. Control schemes for high trajectory (T2) and $\Delta m = 0$

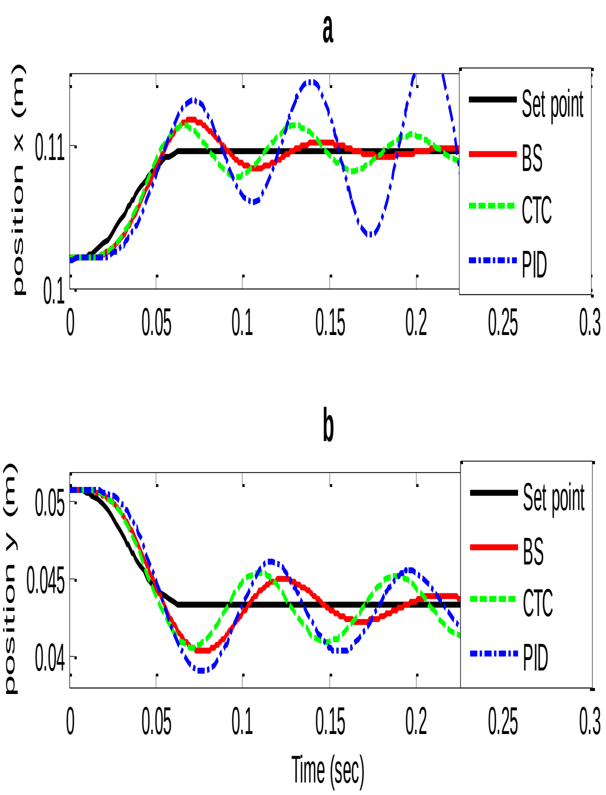

Fig. 7. Control schemes for low trajectory (T1) and $\Delta m = 0.816$

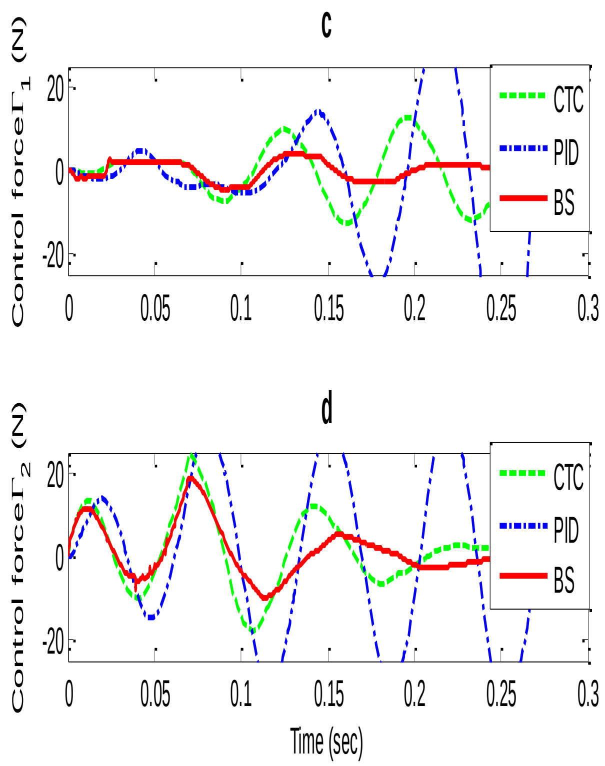

Fig. 8. Control schemes for low trajectory (T1) and $\Delta m = 0.816$

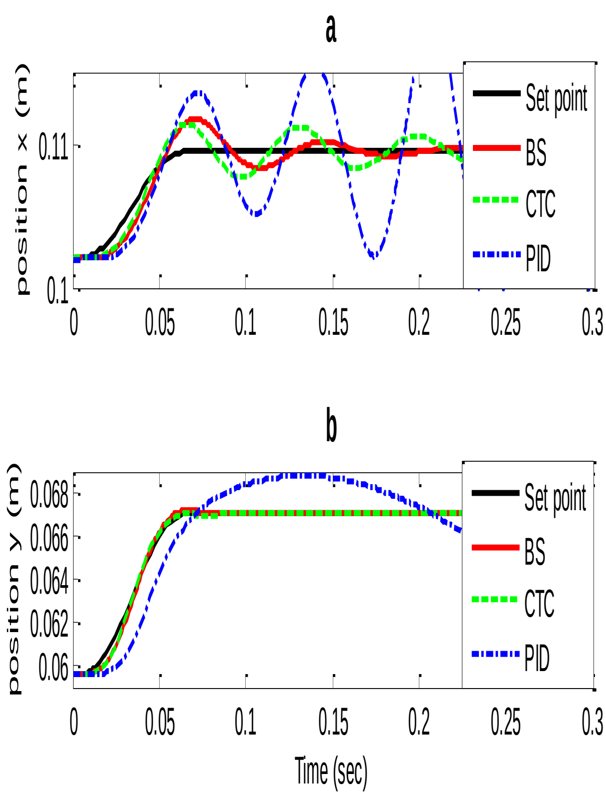

Fig. 9. Control schemes for high trajectory (T2) and $\Delta m = 0.816$

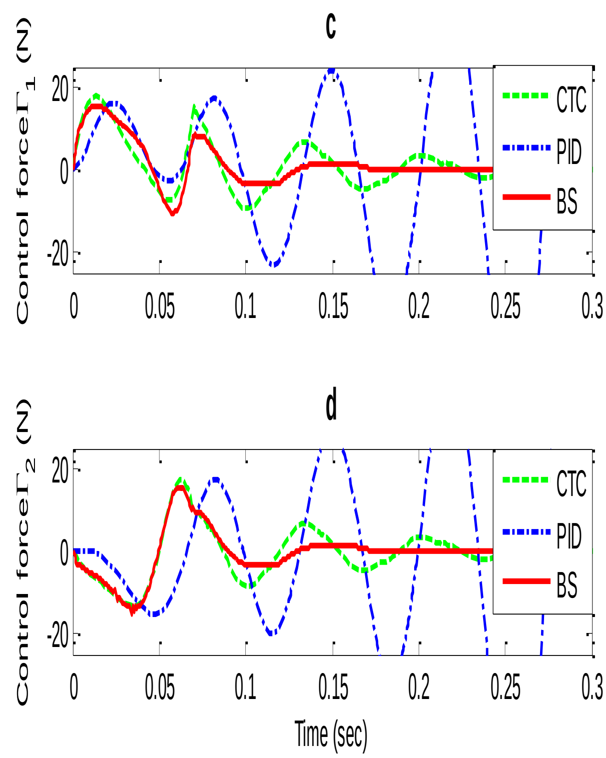

Fig. 10. Control schemes for high trajectory (T2) and $\Delta m = 0.816$

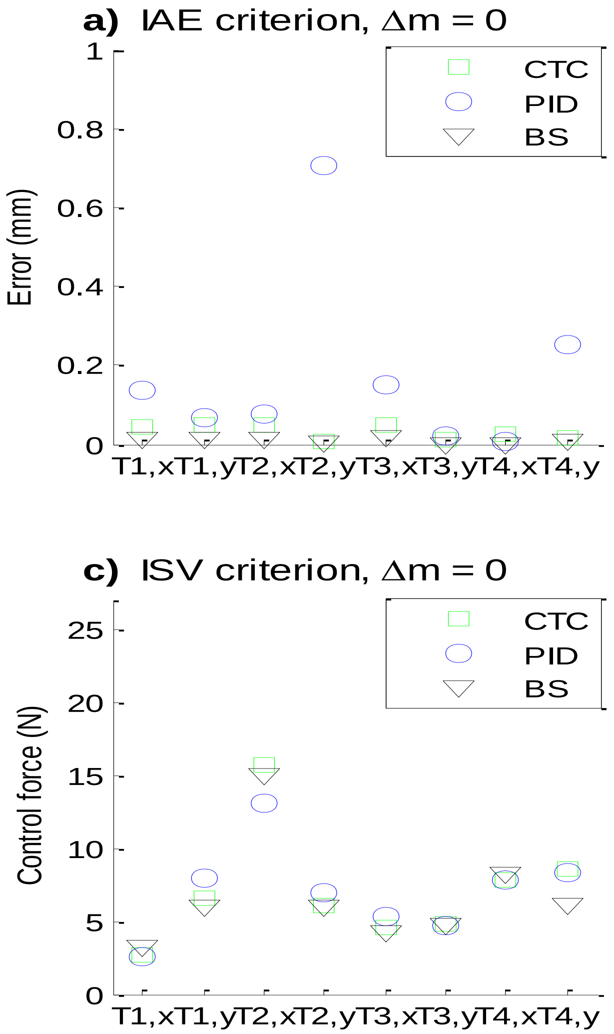

Fig. 11. (a)-(c) Performance criteria (position error and control force) computed for all displacements ($T1\&T4$) trajectories along x and y axes),$\Delta m = 0$

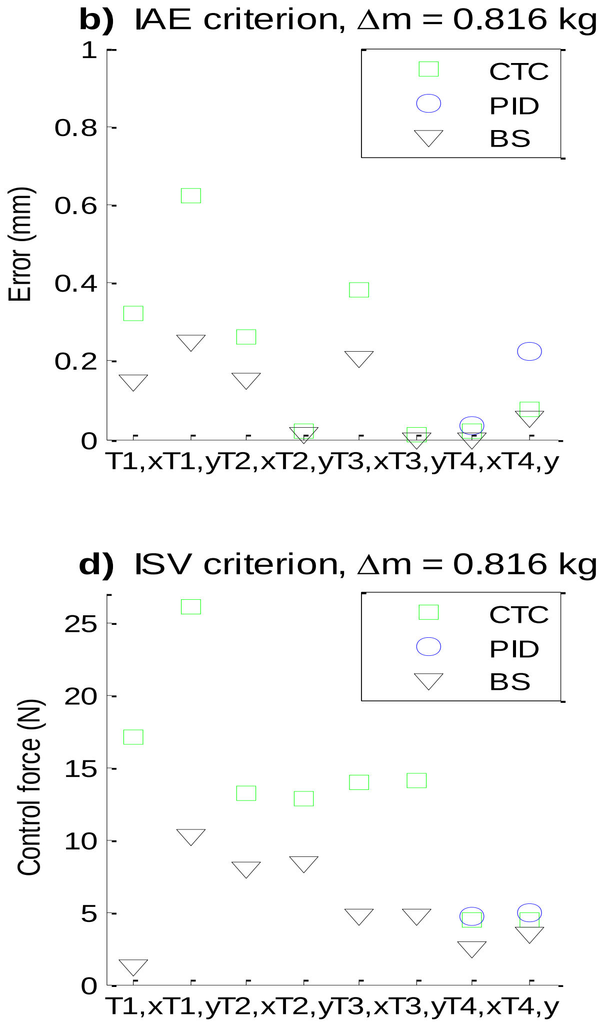

Fig. 12. (b)-(d) Performance criteria (position error and control force) computed for all displacements ($T1\&T4$) trajectories along x and y axes),$\Delta m = 0.816$

presents good results according to structured uncertainties (parametric variation), compared to CTC which presents some oscillation in trajectory response. PID is even worst with unstable closed-loop. In order to quantify the behaviour of the controllers Backstepping, PID and CTC controller, some well-known criteria are computed for 4 trajectories T1, T2, T3 and T4 in the work space Vermeiren et al. (2012). The criteria are computed over a time simulation of $T = 2s$ using the error vector, and the control force input vector.

Based on Figure 11(a) and Figure 12(b), comparison is making for obtained results of error positions. In the different cases ($\Delta m = 0$, $\Delta m = 0.816kg$) the Backstepping controller shows a good trajectories tracking with small error. However, CTC controller presents important position error in trajectories tracking. Meanwhile, PID has unstable behaviour with mass variations. Figure 11(c) and Figure 12(d) present the different results of control force. In the different cases ($\Delta m = 0, \Delta m = 0.816kg$), CTC is much more sensitive to the variation than the Backstepping.

5. CONCLUSION

This paper presents different results of a nonlinear control approach applied to a planar 2DoF parallel manipulator Biglid type. Using Backstepping control approach to achieve a best performance and robust control for trajectory tracking, the control is based on the direct dynamic model in the Cartesian space of the parallel manipulator. The Backstepping is employed successfully for the regulation and tracking of a multi input multi output planer parallel robot in presence of nonlinearities. Asymptotic stability of the closed loop system is established in the Lyapunov sense.

The obtained results for position control problem are rather accepted and the control effort is reasonable.

REFERENCES

Bouabdallah, S. and Siegwart, R. (2007). Full control of a quadrotor. In *Intelligent robots and systems, 2007. IROS 2007. IEEE/RSJ international conference on*, 153–158. IEEE.

Cheung, J.W. and Hung, Y. (2005). Modelling and control of a 2-dof planar parallel manipulator for semiconductor packaging systems. In *Advanced Intelligent Mechatronics. Proceedings, 2005 IEEE/ASME International Conference on*, 717–722. IEEE.

Dawson, D., Carroll, J., and Schneider, M. (1994). Integrator backstepping control of a brush dc motor turning a robotic load. *Control Systems Technology, IEEE Transactions on*, 2(3), 233–244.

Gough, V. (1956). Contribution to discussion of papers on research in automobile stability, control and tyre performance. *Proc. Auto Div. Inst. Mech. Eng*, 171, 392–394.

Guo, Y. and Woo, P.Y. (2003). An adaptive fuzzy sliding mode controller for robotic manipulators. *Systems, Man and Cybernetics, Part A: Systems and Humans, IEEE Transactions on*, 33(2), 149–159.

Hubbard, T., Kujath, M.R., and Fetting, H. (2001). Microjoints, actuators, grippers, and mechanisms. *CCToMM Symposium on Mechanisms, Machines and Mechatronics*.

Kang, B., Chu, J., and Mills, J.K. (2001). Design of high speed planar parallel manipulator and multiple simultaneous specification control. In *Robotics and Automation, 2001. Proceedings 2001 ICRA. IEEE International Conference on*, volume 3, 2723–2728. IEEE.

Kang, B. and Mills, J.K. (2001). Dynamic modeling and vibration control of high speed planar parallel manipulator. In *Intelligent Robots and Systems, 2001. Proceedings. 2001 IEEE/RSJ International Conference on*, volume 3, 1287–1292. IEEE.

Khalil, W. and Ibrahim, O. (2007). General solution for the dynamic modeling of parallel robots. *Journal of intelligent and robotic systems*, 49(1), 19–37.

Le, T.D., Kang, H.J., and Suh, Y.S. (2013). Chattering-free neuro-sliding mode control of 2-dof planar parallel manipulators. *Internation Journal of Advanced Robotic Systems (October 22, 2013)*.

Martynyuk, A. (2000). A survey of some classical and modern developments of stability theory. *Nonlinear Analysis: Theory, Methods & Applications*, 40(1), 483–496.

Merlet, J.P. (2001). *Parallel robots*, volume 74. Springer.

Mustapha, L., Benyamine, A., Abdelhafid, O., Dequidt, A., and Vermeiren, L. (2014). Sliding mode control of biglide planar parallel manipulator. In *Automation and Robotics. Proceedings, 2014 ICINCO International Conference on*, 303–310. ICINCO.

Pierrot, F., Krut, S., Baradat, C., Nabat, V., et al. (2011). Par2: a spatial mechanism for fast planar two-degree-of-freedom pick-and-place applications. *Meccanica*, 46(1), 239–248.

Staicu, S. (2009). Recursive modelling in dynamics of agile wrist spherical parallel robot. *Robotics and Computer-Integrated Manufacturing*, 25(2), 409–416.

Staicu, S., Liu, X.J., and Wang, J. (2007). Inverse dynamics of the half parallel manipulator with revolute actuators. *Nonlinear Dynamics*, 50(1-2), 1–12.

Stewart, D. (1965). A platform with six degrees of freedom. *Proceedings of the institution of mechanical engineers*, 180(1), 371–386.

Su, C.Y. and Stepanenko, Y. (1997). Backstepping-based hybrid adaptive control of robot manipulators incorporating actuator dynamics. *International journal of adaptive control and signal processing*, 11(2), 141–153.

Tsai, L.W. (1999). *Robot analysis: the mechanics of serial and parallel manipulators.* John Wiley & Sons.

Uchiyama, M. (1993). Structures and characteristics of parallel manipulators. *Advanced robotics*, 8(6), 545–557.

Vermeiren, L., Dequidt, A., Afroun, M., and Guerra, T.M. (2012). Motion control of planar parallel robot using the fuzzy descriptor system approach. *ISA transactions*, 51(5), 596–608.

Weck, M. and Staimer, D. (2002). Parallel kinematic machine tools–current state and future potentials. *CIRP Annals-Manufacturing Technology*, 51(2), 671–683.

Yang, Z., Wu, J., and Mei, J. (2007). Motor-mechanism dynamic model based neural network optimized computed torque control of a high speed parallel manipulator. *Mechatronics*, 17(7), 381–390.

Yang, Z., Wu, J., Mei, J., Gao, J., and Huang, T. (2008). Mechatronic model based computed torque control of a parallel manipulator. *International journal of advanced robotic systems*, 5(1), 123–128.

Zhu, X., Tao, G., Yao, B., and Cao, J. (2009). Integrated direct/indirect adaptive robust posture trajectory tracking control of a parallel manipulator driven by pneumatic muscles. *Control Systems Technology, IEEE Transactions on*, 17(3), 576–588.

6. APPENDIX

Numerical simulations include a model with structured and unstructured uncertainties based on the nominal model used to design the controller. Un-modeled dynamics such as elastic joints Vermeiren et al. (2012) between actuators and linkages and Stribeck friction Vermeiren et al. (2012) applied on prismatic joints appear in this augmented model to provide more realistic simulations.

The dynamics of the actuator writes:

$$\Gamma = M_a\ddot{q}_a + b\dot{q}_a + \Gamma_t + \Gamma_f \tag{37}$$

with $q_a = [q_{a1}q_{a2}]^T$, $M_a = diag(m_a m_a)Z$, $\Gamma_f = [\Gamma_{f1}\Gamma_{f2}]^T Z$, the elastic joint model:

$$\Gamma_t = k_t(q_a - q) + b_t(\dot{q}_a - \dot{q}) \tag{38}$$

and the Stribeck friction model of the dry friction:

$$\Gamma_{fi} = \begin{cases} [\Gamma_{fc} + (\Gamma_{fs} - \Gamma_{fc})e^{-(\dot{q}_{ai}/v_s)^2}]sign(\dot{q}_{ai}) \\ if\,|\dot{q}_{ai}| > 0(slip) \\ \min(|\Gamma_i - \Gamma_{ti}|, \Gamma_{fs})sign(\Gamma_i - \Gamma_{ti}) \\ if\,\dot{q}_{ai} = 0(stick) \end{cases} \tag{39}$$

where m_a is the actuator mass, kt k_t the stiffness of the joint, b_t the damping of the joint, Γ_{fs} the static friction force, Γ_{fc} the Coulomb friction force and v_s the sliding speed coefficient.

The linkage and effector dynamics are:

$$\Gamma_t = \hat{M}(P)\ddot{P} + \hat{N}(P,\dot{P}) \tag{40}$$

$$\hat{M}(P) = \begin{pmatrix} m_{L1} + \frac{1}{2}(m - \lambda_1 + \lambda_2) & f_1(P) \\ m_{L2} + \frac{1}{2}(m - \lambda_2 + \lambda_1) & f_2(P) \end{pmatrix}$$

where

$f_1(P) = [(2m_{L1} - 3\lambda_1 - \lambda_2)y^2 + mC(y)^2 + J_1 + J_2]/(2C(y)\cdot y)$

$f_2(P) = [(2m_{L1} - 3\lambda_1 - \lambda_2)y^2 + mC(y)^2 + J_1 + J_2]/(2C(y) \cdot y)$

$$\hat{N}(P, \dot{P}) = \begin{bmatrix} r_{11} & r_{12} \\ r_{21} & r_{22} \end{bmatrix} \dot{P} + p(y)$$

$$\begin{cases} r_{11} = r_{21} \\ r_{12} = -[(2m_{L1} - 3\lambda_1 - \lambda_2)y^2 + (2m_{L1} - 3\lambda_1 - \lambda_2)C(y)^2 + \\ J_1 + J_2]\dot{y}/(2C(y)^3 \\ r_{22} = [(2m_{L2} - 3\lambda_2 - \lambda_1)y^2 + (2m_{L2} - 3\lambda_2 - \lambda_1)C(y)^2 + \\ J_1 + J_2]\dot{y}/(2C(y)^3 \end{cases}$$

where the mass linkage m_{Li} satisfies: $m_i = m_a + m_{Li}, i = 1, 2$.